

Massive Debris Disks May Hinder Secular Stirring by Planetary Companions: An Analytic Proof of Concept

ANTRANIK A. SEFILIAN^{1,2,3}

¹*Astrophysikalisches Institut und Universitätssternwarte, Friedrich-Schiller-Universität Jena, Schillergäßchen 2–3, D-07745 Jena, Germany*

²*Center for Advanced Mathematical Sciences, American University of Beirut, PO Box 11-0236, Riad El-Solh, Beirut 11097 2020, Lebanon*

³*Alexander von Humboldt Postdoctoral Fellow. Email: sefilian.antranik@gmail.com*

Submitted to ApJ

ABSTRACT

Debris disks or exo-Kuiper belts, detected through their thermal or scattered emission from their dusty components, are ubiquitous around main-sequence stars. Since dust grains are short-lived, their sustained presence is thought to require dynamical excitation, i.e., “stirring”, of a massive reservoir of large planetesimals, such that mutual collisions are violent enough to continually supply fresh dust. Several mechanisms have been proposed to explain debris disk stirring, with the commonly accepted being long-term, secular planet-debris disk interactions. However, while effective, existing planet-stirring models are rudimentary; namely, they ignore the (self-)gravity of the disk, treating it as a massless reservoir of planetesimals. Here, using a simple analytical model, we investigate the secular interactions between eccentric planets and massive, external debris disks. We demonstrate that the disk gravity drives fast apsidal precession of both planetesimal and planetary orbits, which, depending on the system parameters, may well exceed the planet-induced precession rate of planetesimals. This results in strong suppression of planetesimal eccentricities and thus relative collisional velocities throughout the disk, often by more than an order of magnitude when compared to massless disk models. We thus show that massive debris disks may hinder secular stirring by eccentric planets orbiting near, e.g., the disk’s inner edge, provided the disk is more massive than the planet. We provide simple analytic formulae to describe these effects. Finally, we show that these findings have important implications for planet inferences in debris-bearing systems, as well as for constraining the total masses of debris disks (as done for β Pic).

Keywords: Exoplanet dynamics (490); Circumstellar disks (235); Debris disks (363); Planetary dynamics (2173)

1. INTRODUCTION

To date, around 20 to 30 per cent of main-sequence stars in the solar neighborhood have been found to harbor belts of debris, akin to Solar System’s asteroid and Kuiper belts (for recent reviews, see, e.g., Hughes et al. 2018; Wyatt 2020). Such debris disks are detected through their excess thermal emission at infrared to millimeter wavelengths, and/or scattered light at optical to near-infrared wavelengths (e.g., Sibthorpe et al. 2018; Esposito et al. 2020). These observations are typically explained by the presence of sub-Earth mass populations of cm-sized and smaller dust grains (e.g., Wyatt & Dent 2002; Holland et al. 2017; Krivov & Wyatt 2021).

The dusty component of debris disks is considered to be of second generation (Wyatt 2008): i.e., generated after the dispersal of protoplanetary disks, rather than being leftover from that phase. This is because dust grains are short-lived compared to the stellar age (Dominik & Decin 2003), as various processes (such as radiation pressure and winds from the host stars) act to clear the dust population (Backman & Paresce 1993). Thus, the sustained presence of dust grains in debris disks is attributed to a “collisional cascade” involving large,

km-sized planetesimals leftover from the protoplanetary disk phase (Wyatt 2008). Within this picture, post-protoplanetary disk dissipation, collisions among large planetesimals generate smaller objects, perpetuating a cascade that continuously supplies fresh dust. To maintain the observed levels of dust, collisional models often require $\sim 10 - 100M_{\oplus}$ in parent planetesimals, and at times, surpassing 10^3M_{\oplus} – a quantity that exceeds the total mass of solids thought to be present during the protoplanetary disk phase. This issue is recognized as the “debris disk mass problem” (Krivov & Wyatt 2021).

For a collisional cascade to be ignited, the reservoir of parent planetesimals needs to satisfy two conditions. First, that parent planetesimals are abundant enough to ensure collisions are frequent, and second, that their orbits are dynamically excited with high enough relative velocities to ensure collisions are destructive (Dohnanyi 1969). While planetesimal formation is an active area of research (e.g., Birnstiel et al. 2016), it is usually assumed that planetesimals form on cold, near-coplanar and circular orbits (e.g., Kenyon & Bromley 2008). Accordingly, it is often thought that additional means of dynamical excitation of planetesimals is re-

quired for debris disks to become visible. This process is referred to as “stirring” in the literature (Wyatt 2008).

Two key mechanisms for stirring have been proposed in the literature, apart from the possibility that debris disks are already *pre-stirred* by processes acting during the protoplanetary disk phase (Wyatt 2008; Matthews et al. 2014). One is known as *self-stirring* (Kenyon & Bromley 2008; Kennedy & Wyatt 2010), whereby planetesimals ignite a collisional cascade due to their gravitational perturbations among each other. This process requires the growth of some planetesimals to a size comparable to Pluto’s, which then dynamically excite the remaining smaller ones. A second mechanism is known as *planet-stirring*, whereby planets excite planetesimal orbits through gravitational interactions, igniting a collisional cascade. Various flavors of this mechanism have been explored, including those examining the long-term, secular perturbations caused by eccentric planets (Mustill & Wyatt 2009), and those focused on short-term perturbations due to circular planets, such as mean-motion resonances and scattering (Costa et al. 2023). In a recent study, Muñoz-Gutiérrez et al. (2023) investigated the synergy of planet- and self-stirring, termed *mixed stirring*, finding enhanced efficiency compared to isolated cases of either mechanism.

Each stirring mechanism comes with its own set of advantages and drawbacks (Wyatt 2008). For instance, while self-stirring does not invoke any planets, it often necessitates considerably large disk masses for optimal efficiency. Indeed, recently, Pearce et al. (2022) have shown that several ALMA-resolved debris disks require masses exceeding $\sim 10^3 M_\oplus$ to be self-stirred. This is deemed to be unfeasible, as such masses exceed the total solid mass thought to be present during the protoplanetary disk phase ($\approx 10^3 M_\oplus$; Krivov & Wyatt 2021). Accordingly, recent studies tend to favor planet-stirring models, in one or another flavor (Pearce et al. 2022; Muñoz-Gutiérrez et al. 2023).

Nevertheless, an important aspect absent in planet-stirring models is the dynamical role of the disk’s gravity, which, in principle may affect the evolution of both the planetesimals and the planet. That is, planet-stirring models often treat the debris disk as a collection of massless planetesimals, solely influenced by the gravitational forces exerted by the star and the (invoked) planets. This raises several questions, motivating the present work: How does the disk gravity affect existing models of planet-stirring, particularly in the context of secular stirring? Can debris particles “resist” planet-stirring through their collective gravity? If so, how does this impact planet inferences derived from simple, massless disk models?

In the realm of protoplanetary disks, studies have already explored somewhat similar questions. For instance, Rafikov (2013a,b) was first to show that massive protoplanetary disks can counteract perturbations due to stellar companions in S- and P-type systems, overcoming the infamous fragmentation barrier by preventing planetesimals from being compelled into highly eccentric and destructive orbits (see also, Silsbee & Rafikov 2015a,b, 2021; Sefilian 2017; Best et al. 2024). A related study by Batygin et al. (2011b) has shown that massive protoplanetary disks can suppress, and in some cases,

inhibit the Kozai-Lidov oscillations expected from a distant stellar companion on an inclined orbit. The common denominator in these studies is the *disk-driven* fast apsidal precession of the planetesimal and/or the stellar companion orbits.

In the realm of debris disks, however, disk gravity is often not considered (e.g., Wyatt et al. 1999; Lee & Chiang 2016; Nesvold et al. 2017; Pearce et al. 2022; Farhat et al. 2023, to name a few). Recently, using (semi-)analytical methods, Sefilian et al. (2021, 2023) presented the first detailed investigation of long-term, secular interactions between eccentric planets and external, *massive* debris disks. They examined scenarios involving disks that are less massive than the planets, finding that a robust outcome is the formation of a wide gap within the disk, giving rise to ‘double-belt’ structures akin to those observed (e.g., Marino 2022). In Sefilian et al. (2021), the authors also noted the potential of relatively massive debris disks to suppress eccentricity excitation due to planets, albeit only in passing.

In this work, motivated by the pioneering works of Rafikov (2013a,b), we propel from the observations made by Sefilian et al. (2021) and show that in single-planet systems with a more massive debris disk than the planet, the disk gravity can reduce planetesimal eccentricities across the disk. Accordingly, the relative velocities at which planetesimals collide are reduced, often by more than an order of magnitude when compared to massless debris disk models. This implies that debris disks, if massive enough, may hinder secular stirring by planetary companions on eccentric orbits. We now describe this idea and its implications in more detail.

2. MODEL SYSTEM

Our general setup is similar to that explored in Sefilian et al. (2021). We consider a coplanar system comprising of a central star of mass M_c , a single planet of mass m_p , and a debris disk of mass M_d situated exterior to the planet (with $m_p, M_d \ll M_c$). The planet’s orbit is assumed to be initially eccentric, characterized by its semimajor axis a_p , eccentricity e_p (typically, $e_p \lesssim 0.1$), and apsidal angle ϖ_p . The debris disk is assumed to be initially circular and axisymmetric. Its inner edge a_{in} is set to be at 5 Hill radii $r_{\text{H,Q}}$ from the planet’s apocenter, $Q_p = a_p(1 + e_p)$, where (Pearce & Wyatt 2014):

$$r_{\text{H,Q}} \approx Q_p \left[\frac{m_p}{(3 - e_p)M_c} \right]^{1/3}, \quad (1)$$

and the outer edge is set at $a_{\text{out}} = 5a_{\text{in}}$. The choice of $a_{\text{in}} = Q_p + 5r_{\text{H,Q}}$ is motivated by the fact that an eccentric planet is expected to clear planetesimals within 5 Hill radii of its apocenter (e.g., Pearce et al. 2024), while $\delta \equiv a_{\text{out}}/a_{\text{in}} = 5$ is chosen to ensure a radially-broad enough disk.

We further characterize the disk’s surface density $\Sigma_d(a)$ by a truncated power-law profile with an exponent p , such that

$$\Sigma_d(a) = \Sigma_0 \left(\frac{a_{\text{out}}}{a} \right)^p \quad (2)$$

for $a_{\text{in}} \leq a \leq a_{\text{out}}$, and $\Sigma_d(a) = 0$ elsewhere. Accordingly, the total mass M_d of the debris disk, given by

$M_d = 2\pi \int_{a_{\text{in}}}^{a_{\text{out}}} a \Sigma_d(a) da$, reads as:

$$M_d = \frac{2\pi}{2-p} \Sigma_0 a_{\text{out}}^2 (1 - \delta^{p-2}). \quad (3)$$

From hereon, we adopt a fiducial disk model with $p = 3/2$, which corresponds to the slope of the Minimum Mass Solar Nebula (Hayashi 1981).

3. BASIC PHYSICS: SECULAR PERTURBATIONS

We are interested in the long-term dynamics of large, \sim km-sized planetesimals initiated on circular orbits within the debris disk. We characterize a planetesimal's orbit with its semimajor axis a , mean motion $n = \sqrt{GM_c/a^3}$, eccentricity e , and apsidal angle ϖ . Given the insensitivity of large planetesimals to radiative non-gravitational forces (Burns et al. 1979), we focus purely on perturbative effects arising due to the gravity of *both* the disk and the planet.

To this end, we follow the calculations presented in Sefilian et al. (2021), performed within the framework of orbit-averaged, secular perturbation theory. Considering the model system of Section 2, Sefilian et al. (2021) presented an analytical expression for the secular disturbing function R – valid to second order in eccentricities¹ – accounting for (i) the disk's gravity, acting *both* on the planet and the planetesimals, and (ii) the planet's gravity acting on the planetesimals; see their Equation (9). These calculations are done by considering the axisymmetric component of the disk gravity, but ignoring its non-axisymmetric contribution. To streamline our conceptual framework presentation, we adhere to this assumption in our present work, reserving the discussion of potential consequences upon its relaxation for Section 6.

Sefilian et al. (2021) then derived the equations of motion describing the evolution of the planetesimal eccentricity vector, namely, $\mathbf{e} = (K, H) = e(\cos \Delta\varpi, \sin \Delta\varpi)$ with $\Delta\varpi \equiv \varpi - \varpi_p$, finding (see also their Equation (10)):

$$\begin{aligned} \frac{dK}{dt} &\approx \frac{-1}{na^2} \frac{\partial R}{\partial H} = -(A - A_{d,p})H, \\ \frac{dH}{dt} &\approx \frac{1}{na^2} \frac{\partial R}{\partial K} = (A - A_{d,p})K + B_p. \end{aligned} \quad (4)$$

These equations of motion are derived in a frame co-precessing with the planetary orbit, thus the definition of \mathbf{e} in terms of $\Delta\varpi$ (rather than ϖ). This is done because the disk gravity causes the planet's apsidal angle to precess linearly in time at a constant rate of $A_{d,p} > 0$, i.e., $\varpi_p(t) = A_{d,p}t + \varpi_p(0)$ (from hereon, $\varpi_p(0) = 0$).

The expressions for the various coefficients appearing in Equation (4) are given in Sefilian et al. (2021, see their Equations (4)–(8)), and we outline them below for completeness.

The term $A_{d,p}$ is given by (see also, Petrovich et al. 2019):

$$\begin{aligned} A_{d,p} &= \frac{3}{4} n_p \frac{2-p}{p+1} \frac{M_d}{M_c} \left(\frac{a_p}{a_{\text{out}}} \right)^3 \frac{\delta^{p+1} - 1}{1 - \delta^{p-2}} \phi_1^c, \\ &\approx 7.04 \times 10^{-1} \text{ Myr}^{-1} \frac{\phi_1^c}{3} \left(\frac{M_d}{1 M_N} \right) \frac{a_{p,30}^{3/2}}{a_{\text{out},150}^3} M_{c,1}^{-1/2}. \end{aligned} \quad (5)$$

In Equation (5), $n_p = \sqrt{GM_c/a_p^3}$ is the planetary mean motion, M_N is Neptune mass, and we have defined: $a_{p,30} \equiv a_p/(30\text{au})$, $a_{\text{out},150} \equiv a_{\text{out}}/(150\text{au})$, and $M_{c,1} \equiv M_c/(1M_\odot)$. The numerical estimate in Equation (5) is for $p = 3/2$ and $\delta = 5$, assuming $a_p/a_{\text{in}} \approx 0.8$ so that $\phi_1^c \approx 3$. Here, ϕ_1^c is a dimensionless factor of order unity given by Equation (A7) in Sefilian et al. (2021); it is a function of a_p/a_{in} that varies very weakly with p and δ (see also their Figure 13). Indeed, irrespective of (p, δ) , one has $\phi_1^c \approx 1$ for $a_p/a_{\text{in}} \ll 1$, and $\phi_1^c \sim 10$ for $a_p/a_{\text{in}} \sim 1$.

In Equation (4), the term $A \equiv A_p + A_d$ represents the free precession rate of the planetesimal, contributed both by the gravity of the planet A_p and the disk A_d . The expression for A_p is given by (see also, Murray & Dermott 1999):

$$\begin{aligned} A_p &= \frac{1}{4} n \frac{m_p}{M_c} \frac{a_p}{a} b_{3/2}^{(1)}(a_p/a), \\ &\approx 1.30 \times 10^{-1} \text{ Myr}^{-1} \left(\frac{m_p}{1 M_N} \right) \frac{a_{p,30}^2}{a_{60}^{7/2}} M_{c,1}^{-1/2}, \end{aligned} \quad (6)$$

where we have defined $a_{60} \equiv a/(60\text{au})$, and A_d reads as:

$$\begin{aligned} A_d &= (2-p)n \frac{M_d}{M_c} \left(\frac{a}{a_{\text{out}}} \right)^{2-p} \frac{\psi_1}{1 - \delta^{p-2}}, \\ &\approx -2.19 \times 10^{-1} \text{ Myr}^{-1} \left| \frac{\psi_1}{-0.55} \right| \left(\frac{M_d}{1 M_N} \right) \frac{a_{60}^{-1}}{a_{\text{out},150}^{1/2}} M_{c,1}^{-1/2}, \end{aligned} \quad (7)$$

see also Silsbee & Rafikov (2015a). In Equation (6), $b_s^{(m)}(\alpha)$ is the standard Laplace coefficient (Murray & Dermott 1999),

$$b_s^{(m)}(\alpha) = \frac{2}{\pi} \int_0^\pi \cos(m\theta) \left(1 + \alpha^2 - 2\alpha \cos \theta \right)^{-s} d\theta, \quad (8)$$

and the numerical estimate assumes $b_{3/2}^{(1)}(\alpha) \approx 3\alpha$, valid for $\alpha \ll 1$. The term ψ_1 appearing in Equation (7) is a dimensionless coefficient of order unity that depends on the disk's surface density slope p and the planetesimal's semimajor axis relative to the disk edges (Silsbee & Rafikov 2015a; Sefilian & Rafikov 2019). For a $p = 3/2$ disk, $\psi_1(a) \approx -0.55$ for $a_{\text{in}} \ll a \ll a_{\text{out}}$, and $\psi_1(a)$ diverges as $a \rightarrow a_{\text{in}}, a_{\text{out}}$. Note that the disk drives retrograde planetesimal precession, $A_d(a) < 0$, opposite to the planet's effect, $A_p(a) > 0$. Moreover, it is important to note that for the particular set of parameters in Equations (5)–(7) with $m_p = M_d$ and $a_p/a_{\text{in}} \approx 0.8$, one has $A_{d,p} \gtrsim |A_d| \gtrsim A_p$.

Finally, the term B_p in Equation (4) represents the excitation of planetesimal eccentricity driven by the eccentric

¹ For a non-linear treatment, valid to fourth order in eccentricities, we refer the reader to, e.g., the study of Sefilian & Touma (2019) concerning the secular interactions between a massive, self-gravitating trans-Neptunian disk and the giant planets in the Solar System (see also, Ward & Hahn 1998).

planet's non-axisymmetric potential. It is given by:

$$B_p = -\frac{1}{4}n \frac{m_p}{M_c} \frac{a_p}{a} b_{3/2}^{(2)}(a_p/a) e_p. \quad (9)$$

Note that the analogous term due to the disk – which may arise once the disk develops some degree of non-axisymmetry – is ignored.

This completes our description of the analytical framework. Before moving on, we remark that this framework is similar to that first developed by Rafikov (2013a,b) for studying the dynamics of planetesimals and its implications for planet formation in stellar binaries (see also, Silsbee & Rafikov 2015a,b, 2021).

4. PLANETESIMAL DYNAMICS IN MASSIVE DISKS

We now analyze the secular dynamics of planetesimals in the combined planet–disk potential. Assuming initially circular orbits for the planetesimals, i.e., $K(0) = H(0) = 0$, Equation (4) admits an analytical solution given by:

$$e(t) = e_m \left| \sin \left(\frac{A_p + A_d - A_{d,p} t}{2} \right) \right|, \quad (10)$$

$$\tan[\Delta\varpi(t)] = \tan \left(\frac{A_p + A_d - A_{d,p} t - \frac{\pi}{2}}{2} \right), \quad (11)$$

where $\Delta\varpi$ stays in the range $[-\pi, \pi]$; see also Equations (11) and (12) in Sefilian et al. (2021). Here, $e_m(a) = 2|e_f(a)|$ is the maximum amplitude of eccentricity oscillations characterized by a period of $T_{\text{osc}} = 2\pi/|A_p + A_d - A_{d,p}|$, where $e_f(a)$ is the forced eccentricity:

$$e_f(a) = \frac{-B_p(a)}{A_p(a) + A_d(a) - A_{d,p}}. \quad (12)$$

Note that in a massless disk one has $A_d = A_{d,p} = 0$, and Equations (10)–(12) reduce to the classical results for test particles perturbed by an eccentric, non-precessing planet (Murray & Dermott 1999). Equations (10)–(12) have been previously utilized by Sefilian et al. (2021) to study planetesimal dynamics in debris disks with $M_d/m_p \lesssim 1$. In the present work, we focus on the case where $M_d/m_p \gtrsim 1$.

4.1. Precession rates

Equations (10)–(12) show that the secular evolution of planetesimals depends on their precession rate $A(a)$ relative to the planet $A_{d,p}$. To assess the disk's contribution, we measure the disk-driven precession rates of planetesimals A_d and the planet $A_{d,p}$ relative to the planet-driven planetesimal precession A_p . Using Equations (5)–(7), we find that:

$$\begin{aligned} \frac{|A_d|}{A_p} &\approx \frac{4|(2-p)\psi_1|}{3(\delta^{2-p}-1)} \frac{M_d}{m_p} \left(\frac{a}{a_{\text{in}}} \right)^{4-p} \left(\frac{a_{\text{in}}}{a_p} \right)^2, \quad (13) \\ &\approx 1.28 \left| \frac{\psi_1}{-0.55} \right| \frac{M_d}{m_p} \left(\frac{a/a_{\text{in}}}{1.5} \right)^{5/2} \left(\frac{a_{\text{in}}/a_p}{1.25} \right)^2, \end{aligned}$$

and

$$\begin{aligned} \frac{A_{d,p}}{A_p} &\approx \frac{(2-p)\phi_1^c}{(p+1)C\delta^3} \frac{M_d}{m_p} \left(\frac{a}{a_{\text{in}}} \right)^{7/2} \left(\frac{a_{\text{in}}}{a_p} \right)^{1/2}, \quad (14) \\ &\approx 2.20 \frac{\phi_1^c}{3} \frac{M_d}{m_p} \left(\frac{a/a_{\text{in}}}{1.5} \right)^{7/2} \left(\frac{a_{\text{in}}/a_p}{1.25} \right)^{1/2}. \end{aligned}$$

Here, the numerical estimates assume $p = 3/2$ and $\delta = 5$ and, for brevity, we have defined $C \equiv (1 - \delta^{p-2})/(\delta^{p+1} - 1)$.

Equations (13) and (14) show that both ratios are increasing functions of a/a_{in} . This holds true for all astrophysically motivated values of p , i.e., $0 < p < 2$, so that more mass is concentrated in the outer parts of the disk than in the inner regions (see Equations (2) and (3)). For the fiducial set of parameters adopted here (Section 2), the disk's gravitational effects would dominate over that due to the planet at distances beyond $a/a_{\text{in}} \sim 1.5$, i.e., $|A_d|/A_p, A_{d,p}/A_p \gtrsim 1$. More specifically, we find that $A_{d,p} \gtrsim |A_d|$ for $a \gtrsim a_c$ where

$$a_c \approx 1.43 a_{\text{in}} \left(\frac{a_{\text{in}}/a_p}{1.25} \right)^{3/2} \left| \frac{\psi_1}{-0.90} \right| \frac{3}{\phi_1^c}, \quad (15)$$

i.e., practically for any $a \gtrsim a_{\text{in}}$ as long as $a_p \sim a_{\text{in}}$.² Within $a \lesssim a_c$, on the other hand, A_p would be the dominant secular frequency, except if $|A_d| > A_p$ which, according to Equation (13) evaluated at $a = a_{\text{in}}$, requires

$$\frac{M_d}{m_p} \gtrsim 1.32 \left| \frac{-0.90}{\psi_1} \right| \left(\frac{a_{\text{in}}/a_p}{1.25} \right)^{-2}. \quad (16)$$

Disk-to-planet mass ratios smaller than that in Equation (16) would lead to the occurrence of secular resonances near $a \approx a_{\text{in}}$ where $A(a) \approx A_p = A_{d,p}$ (Sefilian et al. 2021), and $A_{d,p}$ would dominate the dynamics beyond that location.

To illustrate this further, in Figure 1 we plot the behavior of A_p , $|A_d|$, and $A_{d,p}$ (scaled by n) as a function of planetesimal semimajor axis for several values of M_d/m_p . Calculations assume a Neptune-mass planet at $a_p = 30$ au with $e_p = 0.1$ around a Solar-mass star such that, according to Equation (1), the disk's inner edge is at $a_{\text{in}} \approx 1.25 a_p \approx 37$ au (with $\delta = 5$ and $p = 3/2$; Section 2). Figure 1 shows that for $0.5 \lesssim M_d/m_p \lesssim 10$, the disk-driven planetary precession is indeed the dominant secular frequency beyond $a/a_{\text{in}} \sim 1.5$, such that $A_{d,p} \gtrsim |A_d| \gtrsim A_p$ (in line with Equation (15)). This implies the counter-intuitive result that the disk's gravity acting on the planet is more important than its direct effect on the planetesimals embedded within, i.e., $A_{d,p} \gtrsim |A_d|$. An exception to this can be seen at $a \sim a_{\text{in}}, a_{\text{out}}$ (regardless of M_d/m_p), where $|A_d|$ dominates. This, however, is due to the divergence of $A_d \propto -|\psi_1|$ for $a \rightarrow a_{\text{in}}, a_{\text{out}}$ (Eq. (7); see also Silsbee & Rafikov (2015a); Sefilian & Rafikov (2019)).

Interior to $a/a_{\text{in}} \lesssim 1.5$, Figure 1 shows that the planet-driven planetesimal precession rate dominates over other frequencies such that $A_p \gtrsim A_{d,p}, |A_d|$, i.e., as in the massless

² Note that, in practice, $|\psi_1(a)|$ varies between ≈ 0.95 and ≈ 0.83 within $a/a_{\text{in}} = 1.3$ and 1.4 , which is where $A_{d,p} = |A_d|$ according to Figure 1.

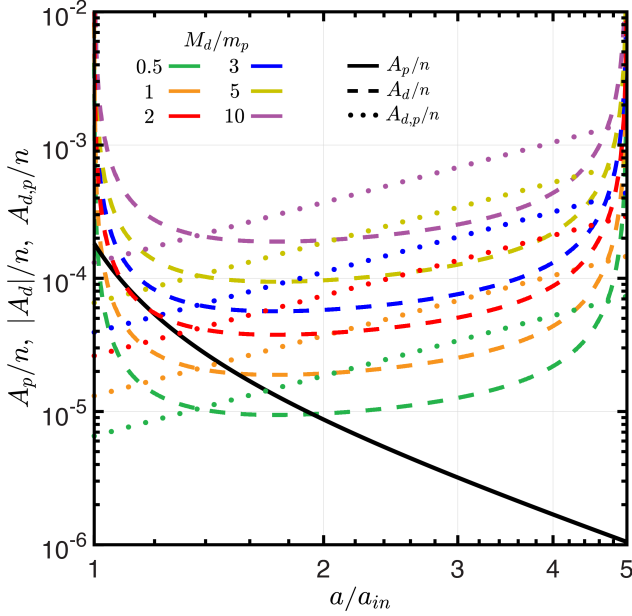


Figure 1. Profiles of the characteristic precession rates in the problem. The plot shows A_p/n (Equation (6); solid black line), $|A_d|/n$ (Equation (7); dashed lines), and $A_{d,p}/n$ (Equation (5); dotted lines), as a function of planetesimal semimajor axis a/a_{in} . Calculations for A_d and $A_{d,p}$ assume different values of M_d/m_p (shown with different colors), assuming $M_c = 1M_\odot$ and a Neptune-mass planet at $a_p = 30$ au with $e_p = 0.1$. The latter sets the disk’s inner at $a_{in} \approx 1.25a_p$ (Equation 1), assumed to have $p = 3/2$ (Equation 2). It is evident that for $M_d/m_p \gtrsim 1$, the disk-driven precession rates dominate throughout the entire disk: namely, $|A_d| \gtrsim A_p$, $A_{d,p}$ within $a/a_{in} \sim 1.5$, and $A_{d,p} \gtrsim |A_d|$, A_p beyond that region.

disk case, only when $M_d/m_p \lesssim 1$ (see also Eq. (16)). The transition from planet- to disk-dominated regimes occurs via a secular resonance where $A_p + A_d = A_{d,p}$ and e_f diverges (see Eq. (12) and Figure 2; Sefilian et al. (2021)). For much more massive disks with $M_d/m_p \gtrsim 1$, on the other hand, Figure 1 shows that the disk-driven planetesimal precession rate A_d (instead of A_p) would be dominant in the innermost regions, $a \lesssim 1.5a_{in}$, in line with Equation (16). This implies that when $M_d/m_p \gtrsim 1$, the relative precession rate of planetesimal orbits would be dominated by the disk gravity alone at all semimajor axes $a_{in} \leq a \leq a_{out}$, while the planet acts only with its non-zero non-axisymmetric torque (i.e., B_p , Eq. (9)). It is this regime that we further explore in this study.

Note that the behavior described above holds as long as $a_p \sim a_{in}$, as would be the case if, e.g., the planet is responsible for sculpting the disk’s inner edge (Equation 1). Otherwise, if $a_p \ll a_{in}$ (not shown in Figure 1), one has $A_{d,p} \propto a_p^{3/2} \rightarrow 0$ (Equation (5)), and the disk-driven planetesimal precession rate $A_d(a)$ (rather than $A_{d,p}$) would dominate beyond some critical semimajor axis. Generally, for a given planet with $a_p/a_{in} \lesssim 1$, this may happen for all values of $M_d/m_p \lesssim 1$. The details of this case are omit-

ted here; for an in-depth exploration, we refer the reader to Sefilian et al. (2021, 2023) and Sefilian (2022).

4.2. Planetesimal eccentricities

Section 4.1 suggests that when considering secular planet-stirring at $a \gtrsim a_{in}$, one can neglect the planetesimal precession due to the planet A_p compared to the disk-driven *planetary* precession $A_{d,p}$ provided that $M_d/m_p \gtrsim 1$ (Equations (15), (16), and Figure 1). Accordingly, Equation (12) predicts that when $A_{d,p} \gg A_p$, $|A_d|$, the forced planetesimal eccentricities $e_f \rightarrow e_f^d$ so that:

$$e_f^d = \left| \frac{B_p}{A_{d,p}} \right| \approx \frac{5(p+1)C}{4|(2-p)|\phi_1^c} e_p \frac{m_p}{M_d} \left(\frac{a_p}{a_{out}} \right)^{3/2} \left(\frac{a_{out}}{a} \right)^{9/2} \quad (17)$$

$$\approx 1.16 \times 10^{-3} \frac{3}{\phi_1^c} \frac{m_p}{M_d} \frac{e_p}{0.10} \frac{a_{p,30}^{3/2} a_{out,150}^3}{a_{100}^{9/2}}.$$

Here, as before, $C = (1 - \delta^{p-2})/(\delta^{p+1} - 1)$, we have approximated $b_{3/2}^{(2)}(\alpha) \approx (15/4)\alpha^2$ (valid for $\alpha \ll 1$), and the numerical estimate assumes $p = 3/2$ and $\delta = 5$. Equation (17) is similar to the one derived by Rafikov (2013a) for planetesimals in massive, circumbinary protoplanetary disks.³

Equation (17) is to be compared with the forced planetesimal eccentricities in a massless disk, in which case $e_f \rightarrow e_f^p$:

$$e_f^p = \left| \frac{B_p}{A_p} \right| = \frac{b_{3/2}^{(2)}(a_p/a)}{b_{3/2}^{(1)}(a_p/a)} e_p \approx \frac{5}{4} \frac{a_p}{a} e_p, \quad (18)$$

$$\approx 3.75 \times 10^{-2} \frac{e_p}{0.10} \frac{a_{p,30}}{a_{100}},$$

see also Mustill & Wyatt (2009). Equations (17) and (18) show that the forced planetesimal eccentricities in massive disks fall off more steeply with semimajor axis than in the massless disk case. Equally important is that massive disks suppress planetesimal eccentricities by more than an order of magnitude compared to massless disks, especially at $a \gg a_p$.

This is illustrated in Figure 2, where we plot the radial profiles of planetesimal forced eccentricities e_f given by Equation (12). Calculations assume the same parameters as in Figure 1. It is evident that for $M_d/m_p \gtrsim 1$, models ignoring the disk’s gravitational effects – so that, $e_f = e_f^p$ (Equation (18); solid black curve in Figure 2) – overestimate the planetesimal eccentricities by more than an order of magnitude throughout nearly the entire disk and $e_f \rightarrow e_f^d$ (Equation (17)). This is true even for disk masses $M_d/m_p \lesssim 1$; however, only in the outer regions of the disk, away from the location of the secular resonance where e_f diverges – see Figure 2 and Sefilian et al. (2021, 2023).

³ An expression that is somewhat similar to Equation (17) is also obtained by Sefilian et al. (2021), however, assuming $|A_d| \gg A_{d,p}$, A_p (rather than $A_{d,p} \gg |A_d|$, A_p as done here). In that case, which is valid for $a_p/a_{in} \ll 1$, one instead finds $e_f^d \propto a_p^3/a^{5-p}$; see their Equation (15).

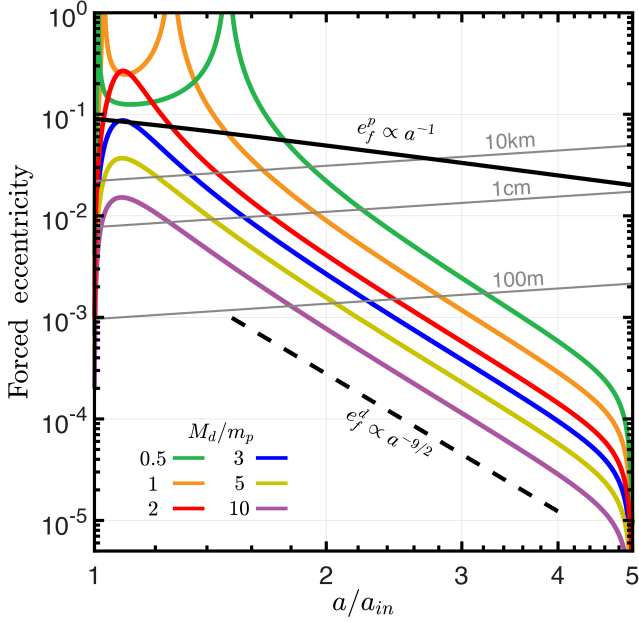


Figure 2. Forced eccentricities of planetesimals $|e_f(a)|$ as a function of their semimajor axis (relative to a_{in}). Calculations are done for different values of M_d/m_p using Equation (12) for the same parameters as in Figure 1. For reference, the black solid line represents the forced eccentricity in a massless disk e_f^p (Equation (18)), and the dashed line illustrates the asymptotic behavior of the eccentricities in massive disks e_f^d (Equation (17)). All of these curves scale linearly with the planetary eccentricity e_p , here taken to be 0.10. The thin gray lines represent the minimum eccentricities e_{stir} for particles of radii 1cm, 100m and 10km to be stirred (Equation (25)). The disk is considered to be unstirred at distances where $|e_f(a)| \lesssim e_{\text{stir}}(1\text{cm})$. See the text (Sections 4.2 and 5) for details.

These findings have important consequences for stirring debris disks as we discuss further in Sections 5 and 6. Before moving on, however, we note that a precessing planet inducing a smaller forced planetesimal eccentricity than a non-precessing one makes intuitive sense. In the extreme case of $\dot{\varpi}_p \rightarrow \infty$, the eccentric planet’s perturbations would reduce to that of a circular planet with an effective semimajor axis of $\approx Q_p$ (Batygin et al. 2011a; Dawson & Murray-Clay 2012).

4.3. Typical evolution/orbit-crossing timescales

Equations (10) and (11) show that the timescale describing the periodic evolution of $e(t)$ and $\Delta\varpi(t)$ is $T_{\text{osc}} = 2\pi/|A_p + A_d - A_{d,p}|$. One can also easily show that T_{osc} is related to the timescales at which debris particles, sharing the same semimajor axis, cross each other’s orbits (e.g., Thébault et al. 2006; Mustill & Wyatt 2009). In the case where the dynamics is dominated by the disk gravity (i.e., $|A_d|, A_{d,p} \gtrsim A_p$), we find that $T_{\text{osc}} \rightarrow T_{\text{osc}}^d$ where:

$$T_{\text{osc}}^d \approx \frac{2\pi}{|A_d(a) - A_{d,p}|} \approx 9 \text{ Myr} \frac{3}{\phi_1^c} \left(\frac{1M_N}{M_d} \right) \frac{a_{\text{out},150}^3}{a_{p,30}^{3/2}} M_{c,1}^{1/2}, \quad (19)$$

for our fiducial system (i.e., $p = 3/2$, $\delta = 5$). Note that the numerical estimate in Equation (19) ignores the contribution of $A_d(a)$ (recall that $|A_d(a)| \lesssim A_{d,p}$; see, e.g., Figure 1). We find that this yields a satisfactory description, generally overestimating the exact value of T_{osc} by a factor of $\lesssim 1.5$, particularly when $a_{\text{in}} \lesssim a \lesssim a_{\text{out}}$, across all systems considered in Figures 1 and 2. Note that the approximation in Equation (19) implies that T_{osc}^d is independent of a ; this holds roughly true even if $A_d(a)$ was not ignored. This is because the disk’s finite extent renders $\psi_1 = \psi_1(a)$ (Silsbee & Rafikov 2015a; Sefilian & Rafikov 2019), causing $|A_d(a)|$ to be slightly shallower than the $\propto a^{-1}$ profile given by the second line of Equation (7). In a massless disk, on the other hand, we find that (see also, e.g., Mustill & Wyatt 2009):

$$T_{\text{osc}} \rightarrow T_{\text{osc}}^p = \frac{2\pi}{A_p(a)} \approx 48 \text{ Myr} \left(\frac{1M_N}{m_p} \right) \frac{a_{60}^{7/2}}{a_{p,30}^2} M_{c,1}^{1/2}. \quad (20)$$

Equations (19) and (20) indicate that debris particles in relatively massive disks evolve, and consequently, cross each other’s orbits more rapidly than in massless disks, particularly at distances $a \gg a_p$. This said, however, we note that the maximum orbital eccentricities attained during the course of the evolution are significantly smaller in massive disks compared to massless disks (Section 4.2).

5. CONSIDERATIONS OF DEBRIS DISK STIRRING

The findings outlined in Section 4 have crucial implications for secular stirring of debris disks by planetary companions, which we now examine in detail.

5.1. Relative collisional and fragmentation velocities

We first analyze the relative collisional velocities between planetesimals and characterize their fragmentation velocities.

Assuming that particles have randomized, uniformly distributed apsidal angles $\Delta\varpi$, the relative collisional velocity between particles can be written as $v_{\text{rel}} = cev_K$, where $v_K = na$ is the local Keplerian orbital velocity, and c is a constant of order unity (Lissauer & Stewart 1993). For values of $c \approx 1.4$ and 2, with $e = |e_f|$ (Equation (12)), v_{rel} could be understood as the mean and maximum relative velocities, respectively (e.g., Mustill & Wyatt 2009).⁴ Given this, we can estimate the mean collisional velocities, $\langle v_{\text{rel}} \rangle$, in a massless disk, i.e., with $e = e_f^p$ (Equation (18)), as follows:

$$\langle v_{\text{rel}}^p \rangle \approx 156 \text{ m.s}^{-1} M_{c,1}^{1/2} a_{100}^{-3/2} a_{p,30} \frac{e_p}{0.10}. \quad (21)$$

In a massive disk ($M_d/m_p \gtrsim 1$), on the other hand, i.e., with $e = e_f^d$ (Equation (17)), we find that:

$$\langle v_{\text{rel}}^d \rangle \approx 4.8 \text{ m.s}^{-1} M_{c,1}^{1/2} \frac{3}{\phi_1^c} \frac{m_p}{M_d} \frac{e_p}{0.10} \frac{a_{p,30}^{3/2} a_{\text{out},150}^3}{a_{100}^5}, \quad (22)$$

⁴ For a Rayleigh distribution of eccentricities, $c = \sqrt{5/4}$ for the mean relative velocities (ignoring inclinations; Ida & Makino 1992). That distribution, however, would arise due to the mutual gravitational scattering of planetesimals, which is different from the secular perturbations we consider. For more details, we refer the reader to Mustill & Wyatt (2009).

assuming the fiducial disk parameters (i.e., $p = 3/2$, $\delta = 5$). Equations (21) and (22) show that the disk gravity lowers the relative collisional velocities of debris particles by more than an order of magnitude, especially at $a \gg a_p$. Such an effect was first pointed out by Rafikov (2013a) in the context of planetesimal dynamics in circumbinary protoplanetary disks.

Generally speaking, collisions lead to fragmentation when the relative collisional velocities exceed a threshold value:

$$v_{\text{rel}} \gtrsim v_{\text{frag}}. \quad (23)$$

In principle, the fragmentation velocity v_{frag} depends on several physical properties of the debris particles, including their radii R_p (e.g., Housen & Holsapple 1990). Here, and in line with previous studies, we define v_{frag} as the minimum velocity at which collisions between particles of *basalt* material and of *similar* radii no longer result in a net gain of mass (e.g., Wyatt & Dent 2002; Krivov et al. 2005, 2018; Costa et al. 2023, and references therein):

$$v_{\text{frag}}(R_p) = 17.5 \text{ m.s}^{-1} \left[\left(\frac{R_p}{\text{m}} \right)^{-0.36} + \left(\frac{R_p}{\text{km}} \right)^{1.4} \right]^{2/3}. \quad (24)$$

This “V”-shaped function has a minimum of $\approx 6.56 \text{ m.s}^{-1}$ at $R_p \approx 112 \text{ m}$, and $v_{\text{frag}}(1 \text{ cm}) \approx v_{\text{frag}}(3.24 \text{ km}) \approx 52.8 \text{ m.s}^{-1}$. It is worth noting that, for the specific set of parameters in Equations (21) and (22), $\langle v_{\text{rel}}^d \rangle$ is lower than the minimum value of $v_{\text{frag}}(R_p)$, in contrast to $\langle v_{\text{rel}}^p \rangle$.

5.2. Critical eccentricity for stirring

We now estimate the minimum eccentricity required to stir debris disks, and compare it to the forced planetesimal eccentricities with and without disk gravity.

To this end, we first translate the fragmentation condition (Equation (23)) into a constraint on the minimum eccentricity, e_{stir} , required for stirring the orbits of debris particles:

$$e_{\text{stir}}(a, R_p) \equiv \frac{v_{\text{frag}}(R_p)}{c v_{\text{K}}(a)} \approx 1.27 \times 10^{-3} M_{c,1}^{-1/2} a_1^{1/2}. \quad (25)$$

In Equation (25), we have used $c \approx 1.4$ (as before), and the numerical estimate assumes $R_p = 1 \text{ cm}$. The latter is chosen because observations probe sub-mm grains, thus larger particles must be destructively colliding for the disk to be stirred and produce the observed dust (see, e.g., Costa et al. 2023). Here, we note that the condition of Equation (25) reduces to the one presented in Costa et al. (2023) upon setting $c = 2$.

As already discussed by Costa et al. (2023), debris particles with eccentricities below $e_{\text{stir}}(a, R_p)$ remain almost certainly unstirred, while those exceeding it might get stirred (depending on $\varpi(a)$, which is not accounted for here; see, e.g., Whitmire et al. (1998)). For reference, the function $e_{\text{stir}}(a, R_p)$ given by Equation (25) is overplotted in Figure 2 for three different values of particle radii: $R_p = 1 \text{ cm}$, 100 m , and 10 km . Looking at Figure 2, it is evident that for $M_d/m_p \gtrsim 1$, the disk’s gravity plays a protective role, preventing destructive collisions among debris particles of various sizes across a substantial portion of the disk’s radial extent. Furthermore, based on the argument that debris disks

will not produce observable dust if $e(a) \lesssim e_{\text{stir}}(1 \text{ cm})$ (Costa et al. 2023), Figure 2 indicates that massive disks would inhibit the expected secular stirring by eccentric planets beyond $a/a_{\text{in}} \sim 1 - 2$, depending on the exact value of M_d/m_p .

5.3. Critical semimajor axis demarcating the disk’s (un)stirred region

We now derive simple analytical formulae to characterize the distances beyond which the disk gravity hinders secular stirring and the production of observable dust.

The critical semimajor axis a_{stir} that demarcates the inner radius of the region where the disk gravity hinders destructive collisions/dust production can be estimated by equating e_f^d and $e_{\text{stir}}(1 \text{ cm})$ (Equations (17) and (25)). Doing so, we find:

$$\begin{aligned} \frac{a_{\text{stir}}^d}{a_{\text{in}}} &\approx 1.43 a_{\text{in},30}^{-1/10} \left[C \frac{p+1}{2-p} \frac{3}{\phi_1^c} \delta^3 \frac{e_p}{0.1} \frac{m_p}{M_d} \left(\frac{a_p}{a_{\text{in}}} \right)^{3/2} M_{c,1}^{1/2} \right]^{1/5} \\ &\approx 1.93 a_{\text{in},30}^{-1/10} \left[\frac{e_p}{0.1} \frac{m_p}{M_d} \left(\frac{a_p/a_{\text{in}}}{0.8} \right)^{3/2} \frac{3}{\phi_1^c} M_{c,1}^{1/2} \right]^{1/5}. \end{aligned} \quad (26)$$

which, for $a_p \sim a_{\text{in}}$ and $M_d/m_p \gtrsim 1$, is comparable to a_{in} . Here, the second line assumes $p = 3/2$ and $\delta = 5$, and it provides a good approximation to the true values of a_{stir} where $e_f = e_{\text{stir}}(1 \text{ cm})$ in Figure 2 (to within $\lesssim 5\%$). Note that according to Equation (26) increasing (decreasing) M_d/m_p at a fixed a_p/a_{in} shifts $a_{\text{stir}}/a_{\text{in}}$ to smaller (larger) values; see also Figure 2. This makes intuitive sense as more massive disks drive faster planetary precession (Equation 5). Equation (26) is to be compared with the massless disk case; setting $e_f^p = e_{\text{stir}}(1 \text{ cm})$, we find that:

$$\frac{a_{\text{stir}}^p}{a_{\text{out}}} \approx 1.18 a_{\text{out},150}^{-1/3} \left[\left(\frac{a_p/a_{\text{in}}}{0.8} \right) \left(\frac{\delta}{5} \right)^{-1} \frac{e_p}{0.1} M_{c,1}^{1/2} \right]^{2/3}, \quad (27)$$

which, for $a_p \sim a_{\text{in}}$, is typically comparable to or larger than $a_{\text{out}} \gtrsim a_{\text{in}}$. Thus, planet-induced secular stirring of debris disks can be severely hindered by the disk’s gravity, provided that $M_d \gtrsim m_p$ for planets near the disk’s inner edge.

5.4. Maximum radius of stirred debris particles

Finally, we compute the maximum sizes $R_{p,\text{max}}$ of debris particles that can be destroyed at a given semimajor axis, both in massless and massive disks.

To this end, we first note that for $R_p \gg 1 \text{ m}$, Equation (24) can be approximated as $v_{\text{frag}} \approx 17.5 \text{ m.s}^{-1} (R_p/\text{km})^{14/15}$. Combining this with the mean relative velocities in a massless disk (Equation (21)), we find that the size of the largest body that can be destroyed by the planet at a given a is:

$$R_{p,\text{max}}^p \approx 18.7 \text{ km} \left[\frac{e_p}{0.1} \left(\frac{a_p/a_{\text{in}}}{0.8} \right) \left(\frac{a/a_{\text{in}}}{2} \right)^{-3/2} \times a_{\text{in},30}^{-1/2} M_{c,1}^{1/2} \right]^{15/14}. \quad (28)$$

Equation (28) closely resembles the one derived by Mustill & Wyatt (2009, Equation (25)); however, there are slight nu-

merical disparities stemming from variations in the definitions of v_{frag} employed (see, e.g., their Equation (22)). In a massive disk, on the other hand, using Equation (22) – which, we remind, assumes $p = 3/2$ and $\delta = 5$ – we find that the largest body that can be destroyed has a radius of

$$R_{p,\text{max}}^d \approx 2.7 \text{ km} \left[\frac{3}{\phi_1^c} \frac{m_p}{M_d} \frac{e_p}{0.1} \left(\frac{a_p/a_{\text{in}}}{0.8} \right)^{3/2} \times \left(\frac{a/a_{\text{in}}}{2} \right)^{-5} a_{\text{in},30}^{-1/2} M_{c,1}^{1/2} \right]^{15/14}. \quad (29)$$

Looking at Equations (28) and (29), one can see that when collisions are destructive, the largest bodies contributing to the collisional cascade are smaller in massive disks compared to those in massless disks, i.e., $R_{p,\text{max}}^d/R_{p,\text{max}}^p \lesssim 1$. This is especially true for debris particles further away from the planet as $R_{p,\text{max}}^d/R_{p,\text{max}}^p \propto (a/a_{\text{in}})^{-7/2}$. This behavior can also be seen by comparing the curves for forced planetesimal eccentricities, i.e., $e_f^d(a)$ and $e_f^p(a)$, with those for $e_{\text{stir}}(R_p)$ in Figure 2, noting that $e_{\text{stir}}(1\text{cm}) \approx e_{\text{stir}}(3.24\text{km})$; see Section 5.1. These findings could have important consequences for modeling of collisional cascades and particle size distributions in debris disks (e.g., Krivov & Wyatt 2021).

6. DISCUSSION AND CONCLUSIONS

Debris disks are often used as probes of exo-planetary systems, as their locations, characteristics and morphologies offer invaluable insights into the presence and properties of planets within their host systems (Hughes et al. 2018; Wyatt 2020). In this spirit, a recent study by Pearce et al. (2022) analyzed a large sample of debris disk-bearing systems (178 in number). Through the application of inner-edge sculpting and secular planet-stirring arguments, the study concluded that the majority of debris disks require \sim Neptune- to Saturn-mass planets within their inner edges, typically at $\sim 10 - 100$ au, with only a few cases requiring \sim Jupiter-mass planets (see, e.g., Figure 14 in Pearce et al. (2022)). While intriguing, the majority of the predicted planets with sub-Jupiter masses remain beyond the reach of current instruments, including JWST (Pearce et al. (2022); see also Carter et al. (2021)).

As discussed in Section 1, planet inferences based on stirring models often use (analytical) models that consider only the gravity of the invoked planet(s), treating the disks as massless entities, as is also done in, e.g., Pearce et al. (2022). The “traditional” planet-stirring mechanism considered in the literature for such purposes is the secular stirring by eccentric planets (Mustill & Wyatt 2009). In this context, however, our results suggest that in systems with more massive debris disks than planets, the secular stirring expected from the planet is reduced, both in severity and radial range, and may even be inhibited across the disk for $M_d/m_p \gg 1$ (Sections 4 and 5). Indeed, if we naively assume that the typical mass of a debris disk is $\sim 100 - 1000M_{\oplus}$ (Krivov & Wyatt 2021), our results imply that the disk cannot be secularly stirred except if the planet is more massive than that, i.e., $\gtrsim 0.3 - 3M_J$, thus surpassing the values predicted for

the majority of planets in Pearce et al. (2022). If true, this implies that there could be many more systems within the sample examined by Pearce et al. (2022) hosting planets with sufficient mass for potential detection.⁵ This should be taken into consideration when, e.g., planning planet observations.

To further illustrate this point, Table 1 lists the values of a_{stir} for six debris-bearing planetary systems assuming $M_d \gtrsim 0$, computed by solving the condition $|e_f(a)| = e_{\text{stir}}(1\text{cm})$ numerically (Section 5.3). Calculations are done adopting the values of m_p and a_p that have been inferred by Pearce et al. (2022) using secular planet-stirring models of *massless* disks (Mustill & Wyatt 2009); see Columns 5 and 6 in Table 1). These combinations of m_p and a_p , together with $e_p = 0.30$ – as stipulated by Pearce et al. (2022) – would stir the disks in Table 1 up to their observed outer edges if $M_d = 0$ (i.e., $|e_f(a)| = e_f^p(a) \gtrsim e_{\text{stir}}(1\text{cm})$ at $a = a_{\text{out}}$ in our notation). It is natural then to ask how this situation would be altered if the disks are assumed to have $M_d \neq 0$. This is shown in Column 7 of Table 1, where we report the minimum and maximum values of a_{stir} corresponding to $M_d = 300M_{\oplus}$ and $30M_{\oplus}$, respectively.⁶ One can see that in all systems, the disk gravity shifts a_{stir} inwards, i.e., closer to a_{in} , and may even inhibit stirring across the entire disk.

Conversely, assuming a maximum disk mass of $M_d = 100M_{\oplus}$ (chosen arbitrarily), we can also compute the minimum planetary masses m_p^{min} required to secularly stir the disks in Table 1. We perform such a calculation such that the disks would be stirred up to⁷ $0.95a_{\text{out}}$; see the last column of Table 1. Comparing m_p^{min} and m_p , it is evident that the planetary masses need to be considerably larger (by up to a factor of ~ 10) than currently thought based on massless disk models. Before moving on, however, we would like to stress that our objective here is not to refine or predict the planetary parameters for these systems, but rather to provide a proof-of-concept illustrating the role of disk gravity.

Taken at face value, the results of preceding sections also imply that if $M_d \gtrsim m_p$, then systems with low, e.g., sub-Saturn mass planets would exhibit an anti-correlation (correlation) with the presence of (relatively narrow) debris disks. Conversely, the presence or future detections of planets in debris-bearing systems can be translated into constraints on the total mass of debris disks for them to be stirred (see Equations (16) and (26)). Indeed, assuming that the observed outer edge of a given disk corresponds to the semi-major axis of the outermost stirred particle, i.e., $a_{\text{stir}} = a_{\text{out}}$, Equation (26) would then yield a *maximum* debris disk mass. Namely, assuming $\delta \gg 1$ and $0 < p < 2$ (i.e., most of the

⁵ For instance, JWST is expected to be sensitive to sub-Jupiter (sub-Saturn) mass planets beyond ~ 30 au (~ 50 au), and as small as $0.1M_J$ at $\gtrsim 100$ au (see, e.g., Carter et al. 2021).

⁶ Note that the systems in Table 1 are shown to require unfeasible disk masses of $\gtrsim 1000M_{\oplus}$ for self-stirring to be efficient (Pearce et al. 2022); values that are much larger than the maximum M_d we consider.

⁷ This is done to prevent the overestimation of m_p^{min} in light of the divergence of A_d at $a = a_{\text{out}}$, which causes $e_f(a_{\text{out}}) \rightarrow 0$; see Figures 1 and 2.

Table 1. Planetary systems with observed debris disks and inferred planets based on secular-stirring arguments.

System	M_c (M_\odot)	t_{age} (Myr)	$[a_{\text{in}}; a_{\text{out}}]$ (au)	m_p (M_J)	a_p (au)	$a_{\text{stir}}^{(a)}$ (au)	m_p^{min} (M_J)
HD 32297	1.68	100	[91; 153]	0.04	70	... – 124.8	0.63
HD 121617	1.90	16	[50; 106]	0.30	37	75.9 – 100.7	1.00
HD 131835	1.81	16	[40; 127]	1.20	30	91.5 – 122	3.24
HD 146181	1.28	16	[70; 90]	0.04	53	... – 78.1	0.35
HD 192425	1.94	400	[100; 420]	0.80	80	212.6 – 332.1	10.65
HD 218396	1.59	42	[170; 210]	0.05	120	... – ...	0.66

NOTE—For each system, the values of M_c , t_{age} , and the disk’s extent, i.e., a_{in} and a_{out} , are taken from [Pearce et al. \(2022\)](#), ignoring the reported observational uncertainties). Columns 5 and 6 present the planetary masses m_p and semimajor axes a_p , as inferred by [Pearce et al. \(2022\)](#), where the authors assume $e_p = 0.30$ based on secular stirring models of *massless* disks ([Mustill & Wyatt 2009](#)). Column 7 presents the minimum and maximum semimajor axis a_{stir} up to which the inferred planets can stir the disks, considering disk masses of $M_d = 300M_\oplus$ and $30M_\oplus$, respectively. Column 8 presents the minimum planetary masses m_p^{min} required to stir the disks, assuming $M_d = 100M_\oplus$. See the text (Section 6) for further details. (a). An empty cell, “...”, indicates that the entire disk remains unstirred.

disk mass is in the outer regions; Equation (2)), we find that $M_d \propto e_p m_p (a_p/a_{\text{in}})^{3/2} / \delta^{3+p}$. The physical significance of such constraints in addressing the “debris disk mass problem” ([Krivov & Wyatt 2021](#)) described in Section 1 would naturally depend on the planetary parameters.

To exemplify this, we consider the β Pic planetary system. According to ALMA observations ([Matrà et al. 2019](#)), its debris disk extends from $a_{\text{in}} \approx 25$ au to $a_{\text{out}} \approx 150$ au (i.e., $\delta \approx 6$). Assuming $p = 3/2$ (Equation (2)), we solve the condition $|e_f(a)| = e_{\text{stir}}(1\text{cm})$ numerically (Section 5.3), finding a maximum disk mass of $M_d \approx 7M_\oplus$ and $\approx 14M_\oplus$ upon stipulating $a_{\text{stir}}/a_{\text{out}} = 0.95$ and 0.90 , respectively. In these simple calculations, we only considered the outer of the two planets in the system, i.e., β Pic b (with $m_p = 9.3M_J$, $a_p = 10.26\text{au}$, $e_p = 0.12$, and $M_c = 1.83M_\odot$; [Brandt et al. \(2021\)](#)), ignoring the presence of β Pic c at ≈ 2.7 au ([Lagrange et al. 2019](#)). Thus, the reported values of M_d serve as a first-order minimum estimate. Remarkably, however, these values of M_d are in agreement with the minimum disk mass estimated by [Krivov & Wyatt \(2021\)](#) – namely, $\approx 5.5M_\oplus$ – based on collisional models assuming the largest planetesimal size is 0.3 km.

Last but not least, it is worth emphasizing that the analytical estimates provided in this paper primarily pertain to radially broad disks with $\delta = a_{\text{out}}/a_{\text{in}} = 5$. However, it is essential to recognize that the fundamental physics extends to wider and even narrower disks, albeit with some simple numerical adjustments. Notably, the disks in Table 1 exhibit δ ranging between ≈ 1.2 to ≈ 4.2 , showcasing the versatility of the considered physics across a spectrum of disk widths. In this regard, the first line of Equation (26) provides a handy tool to gauge the outer boundaries within which secular planet-stirring could be effective in massive debris disks. However, we note that caution must be exercised especially when considering relatively narrow disks ($\delta \approx 1$). This is because mean motion resonances (MMRs), which we have ignored, could play an important dynamical role (see also the

next paragraph), questioning the validity of secular approximation. For instance, for a Jupiter-mass planet, the nominal location of the 2:1 MMR – namely, $a_{2:1} = 2^{2/3}a_p$ (i.e., neglecting potential offsets due to the disk-induced precession; [Murray et al. \(2022\)](#)) – would be within the disk at $a_{2:1}/a_{\text{in}} \approx 1.07$ if $e_p = 0.10$, but $a_{2:1} \lesssim a_{\text{in}}$ if $e_p = 0.30$ (assuming $M_c = 1M_\odot$ and using Equation (1) to relate a_p and a_{in}).

Finally, several factors may influence our conclusions. First, we focused solely on the axisymmetric contribution of the disk gravity, neglecting its non-axisymmetric component. This enabled us to analytically model the disk’s secular effects. While the non-axisymmetric gravitational potential ($\propto B_d$) induced by the debris disk’s eccentricity could theoretically impact the stirring process, we expect minimal influence in the considered regime ($M_d/m_p \gtrsim 1$ and $a_p/a_{\text{in}} \lesssim 1$). This is because, by definition, $B_d \propto e_d$ ([Sillsbee & Rafikov 2015a](#); [Sefilian & Touma 2019](#)), justifying our assumptions when $e_d \sim e_f^d \ll e_p$. The exchange of angular momentum between disk particles (due to $B_d \neq 0$) could, however, cause some departure of $e(a)$ from the $\propto a^{-9/2}$ profile of Equation (17). These issues can be addressed in a computationally effective manner through, e.g., the use of existing orbit-averaged, secular codes designed for simulating the evolution self-gravitating disks. Examples include (i) the Gauss code of [Touma et al. \(2009\)](#), which is valid to all orders of eccentricities and inclinations, and (ii) the linear N-RING code of [Sefilian et al. \(2023\)](#) – valid to second order in eccentricities – based on [Hahn \(2003\)](#). Second, we considered only secular (coplanar) interactions, ignoring the possibility of multiple (possibly inclined) planets, mean motion resonances and scattering with the planet(s), as well as self-stirring. These processes may indeed contribute to the stirring process (as studied in the case of the Kuiper belt, e.g., [Malhotra 1995](#); [Ward & Hahn 1998](#); [Gladman & Chan 2006](#); [Dawson & Murray-Clay 2012](#); [Ribeiro de Sousa et al. 2019](#)), and their collective impact in a self-gravitating disk

warrants further investigation.⁸ Third, we employed a simple collisional and stirring criterion (i.e., Equation (25) with $R_p = 1\text{cm}$); more detailed models (such as those in, e.g., Löhne et al. 2008; Silsbee & Rafikov 2021; Costa et al. 2023) may reveal some differences when compared to our predictions. Fourth and finally, we considered gas-free disks; some debris disks harbor significant amounts of gas (Hughes et al. 2018), which may affect the dynamics considered here. We defer detailed investigation of these issues to future works. Nevertheless, the findings of the present study clearly indicate that disk gravity can significantly impact long-term planet-debris disk interactions, emphasizing the need to address a substantial groundwork in this regard.

To summarize, however, such details are unlikely to undermine the illustrated proof of concept here: relatively massive debris disks – through their axisymmetric gravitational potential – may hinder the expected secular stirring process due to planets on eccentric orbits (e.g., Mustill & Wyatt 2009). At best, this finding holds important implications for planetary inferences derived from stirring analyses of debris disks. At worst, our findings could necessitate adjustments to the masses and orbital parameters of planets invoked to replicate observed levels of stirring, particularly when relying on secular stirring models of massless disks (e.g., Mustill & Wyatt 2009; Pearce et al. 2022). Conversely, if planets are known and/or detected in debris-bearing systems, the findings of this study could be utilized to indirectly measure the total masses of debris disks.

In closing, we remark that the present study is inspired by and hence a variation on the works of Rafikov (2013a,b) concerning planetesimal dynamics in massive, circumstellar/binary protoplanetary disks. Indeed, similar to how massive protoplanetary disks may propel planetesimals past fragmentation barriers and facilitate growth in stellar binaries, massive debris disks may hinder secular stirring by planets and impede dust production through collisions.

ACKNOWLEDGMENTS

A.A.S. is supported by the Alexander von Humboldt Foundation through a Humboldt Research Fellowship for postdoctoral researchers. Back-of-the-envelope calculations for this study were carried out during the Ph.D. research of A.A.S. at DAMTP, University of Cambridge, supported by funding from the Gates Cambridge Trust. The paper was completed during a research visit to Pontificia Universidad Católica de Chile in January 2024, under the generous hosting of Cristobal Petrovich. A.A.S. is grateful to Jihad Touma and Cristobal Petrovich for their engaging discussions and constructive comments on earlier drafts, which significantly improved the overall quality and clarity of the work.

DATA AVAILABILITY

The data supporting the findings of this study are available within the article.

REFERENCES

- Backman, D. E., & Paresce, F. 1993, in *Protostars and Planets III*, ed. E. H. Levy & J. I. Lunine (Tucson, AZ: Univ. Arizona Press), 1253
- Batygin, K., Brown, M. E., & Fraser, W. C. 2011a, *ApJ*, 738, 13, doi: [10.1088/0004-637X/738/1/13](https://doi.org/10.1088/0004-637X/738/1/13)
- Batygin, K., Morbidelli, A., & Tsiganis, K. 2011b, *A&A*, 533, A7, doi: [10.1051/0004-6361/201117193](https://doi.org/10.1051/0004-6361/201117193)
- Best, M., Sefilian, A. A., & Petrovich, C. 2024, *ApJ*, 960, 89, doi: [10.3847/1538-4357/ad0965](https://doi.org/10.3847/1538-4357/ad0965)
- Birnstiel, T., Fang, M., & Johansen, A. 2016, *SSRv*, 205, 41, doi: [10.1007/s11214-016-0256-1](https://doi.org/10.1007/s11214-016-0256-1)
- Brandt, G. M., Brandt, T. D., Dupuy, T. J., Li, Y., & Michalik, D. 2021, *AJ*, 161, 179, doi: [10.3847/1538-3881/abdc2e](https://doi.org/10.3847/1538-3881/abdc2e)
- Burns, J. A., Lamy, P. L., & Soter, S. 1979, *Icarus*, 40, 1, doi: [10.1016/0019-1035\(79\)90050-2](https://doi.org/10.1016/0019-1035(79)90050-2)
- Carter, A. L., Hinkley, S., Bonavita, M., et al. 2021, *MNRAS*, 501, 1999, doi: [10.1093/mnras/staa3579](https://doi.org/10.1093/mnras/staa3579)
- Costa, T., Pearce, T. D., & Krivov, A. V. 2023, *MNRAS*, doi: [10.1093/mnras/stad3582](https://doi.org/10.1093/mnras/stad3582)
- Dawson, R. I., & Murray-Clay, R. 2012, *ApJ*, 750, 43, doi: [10.1088/0004-637X/750/1/43](https://doi.org/10.1088/0004-637X/750/1/43)
- Dohnanyi, J. S. 1969, *J. Geophys. Res.*, 74, 2531, doi: [10.1029/JB074i010p02531](https://doi.org/10.1029/JB074i010p02531)
- Dominik, C., & Decin, G. 2003, *ApJ*, 598, 626, doi: [10.1086/379169](https://doi.org/10.1086/379169)
- Esposito, T. M., Kalas, P., Fitzgerald, M. P., et al. 2020, *AJ*, 160, 24, doi: [10.3847/1538-3881/ab9199](https://doi.org/10.3847/1538-3881/ab9199)
- Farhat, M. A., Sefilian, A. A., & Touma, J. R. 2023, *MNRAS*, 521, 2067, doi: [10.1093/mnras/stad316](https://doi.org/10.1093/mnras/stad316)
- Gladman, B., & Chan, C. 2006, *ApJL*, 643, L135, doi: [10.1086/505214](https://doi.org/10.1086/505214)
- Goldreich, P., & Sari, R. 2003, *ApJ*, 585, 1024, doi: [10.1086/346202](https://doi.org/10.1086/346202)
- Goldreich, P., & Tremaine, S. 1979, *ApJ*, 233, 857, doi: [10.1086/157448](https://doi.org/10.1086/157448)

⁸ Notably, the gravitational coupling between planets and self-gravitating disks at resonances facilitates the exchange of energy and/or angular momentum (Goldreich & Tremaine 1979, 1980). For instance, mean motion or Lindblad resonances may increase the planetary eccentricity $\dot{e}_p \gtrsim 0$ and induce migration toward the star $\dot{a}_p \lesssim 0$ (Goldreich & Sari 2003), while secular resonances may damp e_p without affecting a_p (Tremaine 1998; Ward & Hahn 1998, 2000; Hahn 2008; Sefilian et al. 2023). Such variations in the planetary orbit would then affect the disk stirring levels. Exploring these effects warrants a comprehensive investigation in the future (J. Touma & A. Sefilian, in prep.) and lies beyond the scope of this work.

- . 1980, *ApJ*, 241, 425, doi: [10.1086/158356](https://doi.org/10.1086/158356)
- Hahn, J. M. 2003, *ApJ*, 595, 531, doi: [10.1086/377195](https://doi.org/10.1086/377195)
- . 2008, *ApJ*, 680, 1569, doi: [10.1086/588019](https://doi.org/10.1086/588019)
- Hayashi, C. 1981, *Progress of Theoretical Physics Supplement*, 70, 35, doi: [10.1143/PTPS.70.35](https://doi.org/10.1143/PTPS.70.35)
- Holland, W. S., Matthews, B. C., Kennedy, G. M., et al. 2017, *MNRAS*, 470, 3606, doi: [10.1093/mnras/stx1378](https://doi.org/10.1093/mnras/stx1378)
- Housen, K. R., & Holsapple, K. A. 1990, *Icarus*, 84, 226, doi: [10.1016/0019-1035\(90\)90168-9](https://doi.org/10.1016/0019-1035(90)90168-9)
- Hughes, A. M., Duchêne, G., & Matthews, B. C. 2018, *ARA&A*, 56, 541, doi: [10.1146/annurev-astro-081817-052035](https://doi.org/10.1146/annurev-astro-081817-052035)
- Ida, S., & Makino, J. 1992, *Icarus*, 96, 107, doi: [10.1016/0019-1035\(92\)90008-U](https://doi.org/10.1016/0019-1035(92)90008-U)
- Kennedy, G. M., & Wyatt, M. C. 2010, *MNRAS*, 405, 1253, doi: [10.1111/j.1365-2966.2010.16528.x](https://doi.org/10.1111/j.1365-2966.2010.16528.x)
- Kenyon, S. J., & Bromley, B. C. 2008, *ApJS*, 179, 451, doi: [10.1086/591794](https://doi.org/10.1086/591794)
- Krivov, A. V., Ide, A., Löhne, T., Johansen, A., & Blum, J. 2018, *MNRAS*, 474, 2564, doi: [10.1093/mnras/stx2932](https://doi.org/10.1093/mnras/stx2932)
- Krivov, A. V., Sremčević, M., & Spahn, F. 2005, *Icarus*, 174, 105, doi: [10.1016/j.icarus.2004.10.003](https://doi.org/10.1016/j.icarus.2004.10.003)
- Krivov, A. V., & Wyatt, M. C. 2021, *MNRAS*, 500, 718, doi: [10.1093/mnras/staa2385](https://doi.org/10.1093/mnras/staa2385)
- Lagrange, A. M., Meunier, N., Rubini, P., et al. 2019, *Nature Astronomy*, 3, 1135, doi: [10.1038/s41550-019-0857-1](https://doi.org/10.1038/s41550-019-0857-1)
- Lee, E. J., & Chiang, E. 2016, *ApJ*, 827, 125, doi: [10.3847/0004-637X/827/2/125](https://doi.org/10.3847/0004-637X/827/2/125)
- Lissauer, J. J., & Stewart, G. R. 1993, in *Protostars and Planets III*, ed. E. H. Levy & J. I. Lunine, 1061
- Löhne, T., Krivov, A. V., & Rodmann, J. 2008, *ApJ*, 673, 1123, doi: [10.1086/524840](https://doi.org/10.1086/524840)
- Malhotra, R. 1995, *AJ*, 110, 420, doi: [10.1086/117532](https://doi.org/10.1086/117532)
- Marino, S. 2022, arXiv e-prints, arXiv:2202.03053, doi: [10.48550/arXiv.2202.03053](https://doi.org/10.48550/arXiv.2202.03053)
- Matrà, L., Wyatt, M. C., Wilner, D. J., et al. 2019, *AJ*, 157, 135, doi: [10.3847/1538-3881/ab06c0](https://doi.org/10.3847/1538-3881/ab06c0)
- Matthews, B. C., Krivov, A. V., Wyatt, M. C., Bryden, G., & Eiroa, C. 2014, in *Protostars and Planets VI*, ed. H. Beuther, R. S. Klessen, C. P. Dullemond, & T. Henning, 521–544, doi: [10.2458/azu_uapress.9780816531240-ch023](https://doi.org/10.2458/azu_uapress.9780816531240-ch023)
- Muñoz-Gutiérrez, M. A., Marshall, J. P., & Peimbert, A. 2023, *MNRAS*, 520, 3218, doi: [10.1093/mnras/stad218](https://doi.org/10.1093/mnras/stad218)
- Murray, C. D., & Dermott, S. F. 1999, *Solar System Dynamics* (Cambridge: Cambridge Univ. Press)
- Murray, Z., Hadden, S., & Holman, M. J. 2022, *ApJ*, 931, 66, doi: [10.3847/1538-4357/ac68f2](https://doi.org/10.3847/1538-4357/ac68f2)
- Mustill, A. J., & Wyatt, M. C. 2009, *MNRAS*, 399, 1403, doi: [10.1111/j.1365-2966.2009.15360.x](https://doi.org/10.1111/j.1365-2966.2009.15360.x)
- Nesvold, E. R., Naoz, S., & Fitzgerald, M. P. 2017, *ApJL*, 837, L6, doi: [10.3847/2041-8213/aa61a7](https://doi.org/10.3847/2041-8213/aa61a7)
- Pearce, T. D., & Wyatt, M. C. 2014, *MNRAS*, 443, 2541, doi: [10.1093/mnras/stu1302](https://doi.org/10.1093/mnras/stu1302)
- Pearce, T. D., Launhardt, R., Ostermann, R., et al. 2022, *A&A*, 659, A135, doi: [10.1051/0004-6361/202142720](https://doi.org/10.1051/0004-6361/202142720)
- Pearce, T. D., Krivov, A. V., Sefilian, A. A., et al. 2024, *MNRAS*, 527, 3876, doi: [10.1093/mnras/stad3462](https://doi.org/10.1093/mnras/stad3462)
- Petrovich, C., Wu, Y., & Ali-Dib, M. 2019, *AJ*, 157, 5, doi: [10.3847/1538-3881/aaeed9](https://doi.org/10.3847/1538-3881/aaeed9)
- Rafikov, R. R. 2013a, *ApJL*, 764, L16, doi: [10.1088/2041-8205/764/1/L16](https://doi.org/10.1088/2041-8205/764/1/L16)
- . 2013b, *ApJL*, 765, L8, doi: [10.1088/2041-8205/765/1/L8](https://doi.org/10.1088/2041-8205/765/1/L8)
- Ribeiro de Sousa, R., Gomes, R., Morbidelli, A., & Vieira Neto, E. 2019, *Icarus*, 334, 89, doi: [10.1016/j.icarus.2018.08.008](https://doi.org/10.1016/j.icarus.2018.08.008)
- Sefilian, A. A. 2017, Master's thesis, American University of Beirut, Lebanon, doi: <http://hdl.handle.net/10938/21103>
- . 2022, PhD thesis, University of Cambridge, UK, doi: [10.17863/CAM.84460](https://doi.org/10.17863/CAM.84460)
- Sefilian, A. A., & Rafikov, R. R. 2019, *MNRAS*, 489, 4176, doi: [10.1093/mnras/stz2412](https://doi.org/10.1093/mnras/stz2412)
- Sefilian, A. A., Rafikov, R. R., & Wyatt, M. C. 2021, *ApJ*, 910, 13, doi: [10.3847/1538-4357/abda46](https://doi.org/10.3847/1538-4357/abda46)
- . 2023, *ApJ*, 954, 100, doi: [10.3847/1538-4357/ace68e](https://doi.org/10.3847/1538-4357/ace68e)
- Sefilian, A. A., & Touma, J. R. 2019, *AJ*, 157, 59, doi: [10.3847/1538-3881/aaf0fc](https://doi.org/10.3847/1538-3881/aaf0fc)
- Sibthorpe, B., Kennedy, G. M., Wyatt, M. C., et al. 2018, *MNRAS*, 475, 3046, doi: [10.1093/mnras/stx3188](https://doi.org/10.1093/mnras/stx3188)
- Silsbee, K., & Rafikov, R. R. 2015a, *ApJ*, 798, 71, doi: [10.1088/0004-637X/798/2/71](https://doi.org/10.1088/0004-637X/798/2/71)
- . 2015b, *ApJ*, 808, 58, doi: [10.1088/0004-637X/808/1/58](https://doi.org/10.1088/0004-637X/808/1/58)
- . 2021, *A&A*, 652, A104, doi: [10.1051/0004-6361/202141139](https://doi.org/10.1051/0004-6361/202141139)
- Thébault, P., Marzari, F., & Scholl, H. 2006, *Icarus*, 183, 193, doi: [10.1016/j.icarus.2006.01.022](https://doi.org/10.1016/j.icarus.2006.01.022)
- Touma, J. R., Tremaine, S., & Kazandjian, M. V. 2009, *MNRAS*, 394, 1085, doi: [10.1111/j.1365-2966.2009.14409.x](https://doi.org/10.1111/j.1365-2966.2009.14409.x)
- Tremaine, S. 1998, *AJ*, 116, 2015, doi: [10.1086/300567](https://doi.org/10.1086/300567)
- Ward, W. R., & Hahn, J. M. 1998, *AJ*, 116, 489, doi: [10.1086/300398](https://doi.org/10.1086/300398)
- Ward, W. R., & Hahn, J. M. 2000, in *Protostars and Planets IV*, ed. V. Mannings, A. P. Boss, & S. S. Russell (Tucson, AZ: Univ. Arizona Press), 1135
- Whitmire, D. P., Matese, J. J., Criswell, L., & Mikkola, S. 1998, *Icarus*, 132, 196, doi: [10.1006/icar.1998.5900](https://doi.org/10.1006/icar.1998.5900)
- Wyatt, M. 2020, *Extrasolar Kuiper belts* (Oxford: Elsevier), 351–376, doi: [10.1016/B978-0-12-816490-7.00016-3](https://doi.org/10.1016/B978-0-12-816490-7.00016-3)
- Wyatt, M. C. 2008, *ARA&A*, 46, 339, doi: [10.1146/annurev.astro.45.051806.110525](https://doi.org/10.1146/annurev.astro.45.051806.110525)
- Wyatt, M. C., & Dent, W. R. F. 2002, *MNRAS*, 334, 589, doi: [10.1046/j.1365-8711.2002.05533.x](https://doi.org/10.1046/j.1365-8711.2002.05533.x)
- Wyatt, M. C., Dermott, S. F., Telesco, C. M., et al. 1999, *ApJ*, 527, 918, doi: [10.1086/308093](https://doi.org/10.1086/308093)